JSHC
Japan Society of Histochemistry and Cytochemistry
Established 1959

Acta Histochem. Cytochem. 44 (6): 247–258, 2011
doi:10.1267/ahc.11033

ASURA (PHB2) Is Required for Kinetochore Assembly and Subsequent Chromosome Congression

Mei Hann Lee[1], Linyen Lin[2], Ilma Equilibrina[1], Susumu Uchiyama[1], Sachihiro Matsunaga[1,3] and Kiichi Fukui[1]

[1]Department of Biotechnology, Graduate School of Engineering, Osaka University, GSE Common East 7 F, 2–1 Yamadaoka, Suita, Osaka 565–0871, Japan, [2]Research Center for Ultra-High Voltage Electron Microscopy, Osaka University, 7–1, Mihogaoka, Ibaraki, Osaka 567–0047, Japan and [3]Present address: Department of Applied Biological Science, Faculty of Science and Technology, Tokyo University of Science, 2641 Yamazaki, Noda, Chiba 278–8510, Japan

Received July 7, 2011; accepted August 25, 2011; published online October 22, 2011

ASURA (PHB2) knockdown has been known to cause premature loss of sister chromatid cohesion, and disrupt the localization of several outer plate proteins to the kinetochore. As a result, cells are arrested at mitotic phase and chromosomes fail to congress to the metaphase plate. In this study, we further clarified the mechanism underlying ASURA function on chromosome congression. Interestingly, ASURA is not specifically localized at the kinetochore during mitotic phase, unlike other kinetochore proteins which construct the kinetochore. Electron microscopy (EM) observation showed that ASURA is required for proper kinetochore formation. By the partial depletion of ASURA, kinetochore maturation is impaired, and kinetochores showing fibrillar balls without a well-defined outer plates are often observed. Moreover, even when the outer plates of kinetochores are constructed, most showed structures stretched and/or distended from the centromere, which resembled premature kinetochores at prometaphase, indicating that the constructed kinetochore plates are less rigid against tension derived from kinetochore microtubule pulling forces. We concluded that ASURA is an essential protein for complete kinetochore development, although ASURA is not being integrated to the kinetochore. These results highlight the uniqueness of ASURA as a kinetochore protein.

Key words: ASURA, PHB2, kinetochore assembly, chromosome congression, electron microscopy

I. Introduction

Proper chromosome segregation requires a faithful physical link between spindle microtubules (MTs) and centromeric DNA via a protein supercomplex called the kinetochore [10]. Accumulating strands of evidence reveal that the kinetochore performs at least four functions. In addition to the well-known role as a chromosomal attachment site for spindle MTs during cell division [4, 38], the kinetochore is also a complex machine that exerts the force for poleward chromosome motion [35, 39], while simultaneously controlling the dynamics of its associated MTs [33, 51], and generating the cell-cycle checkpoint that delays anaphase onset until all chromosomes are bioriented and aligned at the spindle equator [46].

Kinetochore is a trilaminar structural body revealed by electron microscopic studies [3, 11], and was shown to be visible only during mitosis [40]. Kinetochore morphogenesis has been well documented for mammalian cells [38], especially in PtK [40]. Biochemical analysis together with correlative light microscopy and EM provided crucial insights into kinetochore assembly. From a structural viewpoint, during mitosis, the kinetochore is visible on the surface of the primary constrictions as roughly circular patches of fine fibrillar materials (fibrillar ball), which

Correspondence to: Prof. Kiichi Fukui, Department of Biotechnology, Graduate School of Engineering, Osaka University, GSE Common East 7 F, 2–1 Yamadaoka, Suita, Osaka 565–0871, Japan.
E-mail: kfukui@bio.eng.osaka-u.ac.jp

gradually differentiates into two layers within the ball and develops finally into the trilaminar morphology. This layered structure is reflected by its molecular mean. CENP-A, CENP-B and other CCAN (constitutive centromere-associated network) proteins reside throughout the cell cycle [9, 16]. Pools of proteins for the kinetochore outer plate and the corona, as well as the spindle checkpoint components gradually localize at the kinetochore since G2-phase and the trilaminar structure is established [9, 25]. Thanks to the continuing effort to elucidate the kinetochore components [1, 7, 8, 36] by fluorescence microscopy [20, 37, 50], electron microscopic study [14, 25], and biochemical means [9], over 120 components constituting the molecular architecture of kinetochore [41] have been reported to date. In-depth insight into their contributions to kinetochore assembly and function have also emerged. Nonetheless, the mechanisms of kinetochore maturation, that is, how pre-kinetochores assemble into the mature three-layer structure, remain largely uncharacterized.

Prohibitins (PHBs) are reported to implicate cell cycle progression, transcriptional regulation, cellular signaling, apoptosis and mitochondrial biogenesis, and mitochondrial cristae morphogenesis [31]. PHB1 (prohibitin 1) and PHB2 (prohibitin 2 or prohibitone) assemble into a ring-like macromolecular complex mainly localized to the mitochondrial inner membrane [2, 29]. Although subcellular localization of PHBs has been confined to mitochondria, a nuclear localization of PHBs also has been reported [18, 47]. Human PHB2 is involved as a repressor of nuclear estrogen receptor activity, and was found to be identical to REA (repressor of estrogen receptor activity) [34], a histone deacetylase interacting partner that modulates the activity of a defined subset of nuclear hormone receptors in rat, mouse, and human cell lines [23]. In HeLa cells, PHB2 is translocated into the nucleus in the presence of ERα (estrogen receptor alpha) and E2 (estradiol) where it interacts with and inhibits the transcriptional activity of the ER [22]. Besides these early reports, we previously revealed that PHB2, which was identified as a metaphase chromosome component in chromosome proteome analysis [44, 49] and is essential for the protection of sister chromatid cohesion, is required for mitotic spindle formation and localization of several kinetochore proteins [45]. Because of its multifunctional roles, we termed PHB2 (identical to REA) as 'ASURA' in the rest of this manuscript, which is named after the fierce Buddhist demigod that has three faces and six arms demonstrating its multiple functions. In this electron microscopic study, we uncovered a new function of ASURA in ensuring proper kinetochore formation.

II. Materials and Methods

Cell culture

HeLa cells were maintained in Dulbecco's modified Eagle's medium (DMEM; GIBCO BRL) supplemented with 10% fetal-bovine serum (FBS; Equitech-Bio) at 37°C and 5% CO_2.

Antibodies

The following antibodies were used in immunofluorescence microscopy and immunoblotting. A rabbit ASURA polyclonal antibody was generated as described previously [45] and used at a dilution of 1:1000. The other primary antibodies were anti-CENP-F rabbit polyclonal (1:2000, Novus Biologicals), anti-Hec1 mouse monoclonal (1:1000, Affinity Bioreagents), anti-CREST (1:1000, Cortex Biochem), and anti-α-tubulin mouse monoclonal (1:500, Calbiochem). Secondary antibodies for immunoblot analyses are alkaline phosphatase anti-mouse IgG (1:2000, Vector Laboratories) and alkaline phosphatase anti-rabbit IgG (1:2000, Vector Laboratories). For immunofluorescence analyses, secondary antibodies were Alexa Fluor 488 anti-mouse monoclonal (1:500, Molecular Probes), Alexa Fluor 488 anti-rabbit monoclonal (1:500, Molecular Probes), and anti-human IgG (1:200, Sigma).

siRNA methods

HeLa cells were transfected using Lipofectamine 2000 (Invitrogen) according to the manufacturer's instructions at a final concentration of 100 nM with ASURA-siRNA (PHB2 siRNA-1 in [45]) or Hec1 siRNA (5'-AAGTTCAAAAGCT GGATGATC-3') [27]. Cells transfected with Lipofectamine alone were used as a control. Cells were collected 48 hr post-transfection for use in analysis.

Immunoblotting and gel electrophoresis

Cells (siRNA or mock transfected) grown in 24-well plates were collected and lysed in 2× Laemmli Sample Buffer (Santa Cruz Biotechnology) with an equal amount of PBS buffer. Protein extracts were fractionated on 10% polyacrylamide gels and then transferred onto PVDF membrane. The immunoblots were blocked with 1% BSA-TBST (0.1% Tween 20, 25 mM Tris-HCl pH 7.4, 137 mM NaCl, 25 mM KCl) and labeled with the primary and secondary antibodies. The immunoreactive protein bands were detected by NBT/BCIP solution (Roche) diluted in AP buffer (100 mM Tris-HCl, pH 9.5, 100 mM NaCl, 1 mM $MgCl_2$).

Immunofluorescence microscopy

HeLa cells grown on coverslips were transfected with target siRNA, fixed with 4% PFA (*para*-formaldehyde) diluted in PBS (phosphate buffered saline, pH 7.4) for 15 min at 37°C, and stained with Hoechst 33342 (Sigma) for mitotic index calculation. For proteins localization analyses, cells were fixed either with 4% PFA containing 0.5% Triton X-100 diluted in PBS for 15 min (for Hec1 and CREST staining) or 100% ice-cold methanol for 10 min at –20°C (for CENP-F and CREST staining). Alternatively, cells were arrested at metaphase by adding colcemid (final concentration 0.1 μg/ml) in the culture medium for 3 hr at 37°C and were collected for metaphase-chromosome spreads as described earlier [26]. Cells were blocked with 1% BSA in PBS at room temperature for 30 min. Then, primary and secondary antibody interactions were carried out for 1 hr at room temperature, respectively. Samples were then mounted

in Vectorshield mounting medium (Vector Laboratories) and examined under an Axioplan II imaging fluorescence microscope (Carl Zeiss) equipped with a CCD camera (MicroMax, Roper Scientific) driven by the IP Lab software.

Electron microscopy

HeLa cells transfected as above for 48 hr were later fixed in 3% glutaraldehyde and 0.2% tannic acid diluted in PBS buffer for 1 hr at room temperature. Post-fixation was in 2% OsO_4 for 20 min. The cells were dehydrated through an increasing ethanol series and infiltrated with epoxy resin (Quetol 812). The resin was polymerized at 37°C for 12 hr, 45°C for 12 hr and 60°C for 48 hr. Cells of interest embedded in the resin were chosen under an optical microscope and trimmed to ~1.0 mm^2. Samples were cut into 70–80 nm thick serial sections with an ultramicrotome equipped with a diamond knife (Ultracut E, Reichart-Jung). The sections were stained with uranyl acetate and lead citrate for examination with a transmission electron microscope (JEM-1200EX, JOEL).

Our EM analyses are based on those of DeLuca *et al.* [13] with some alterations. For control, cells that apparently aligned at metaphase plate were chosen for analysis. ASURA and Hec1 RNAi cells were chosen based on their phenotypes of poor chromosome alignment. All kinetochores observed were included in the analyses regardless of their appearance. For individual cells, only a few sections, containing chromosome-rich regions, which were often close to the center of the cells, were examined. As the boundary between individual chromosomes is not obvious, and sister kinetochore appearances can sometimes show differences depending on kinetochore fiber attachment, kinetochores were analyzed individually rather than as a kinetochore pair of a chromosome. Furthermore, as kinetochore morphology varies even between adjacent serial sections, which has also been reported for Indian muntjac chromosomes [53], we analyzed several adjacent serial sections to classify individual kinetochores. Kinetochore is classified as trilaminar once the canonical layered structure is visible in any of the adjacent serial sections for an individual kinetochore, even if the structure is rather fuzzy in other sections.

III. Results

Mitotic progression was impaired by partial depletion of ASURA

To test how ASURA functions in mitosis, we transfected HeLa cells with a 21-nucleotide duplex homologous to a portion of the ASURA sequence. As a result, ASURA expression levels were strongly reduced 48 hr after transfection (26% of control) as shown in Figure 1A. Further observation revealed a significant increase in mitotic index to about 3-fold that of the control (4.7±0.3%) in ASURA RNAi cultures (13.4±1.9%) (Fig. 1B). We previously showed that ASURA RNAi affected the kinetochore localization of several kinetochore proteins, including Hec1 [45]. Thus, we checked the effects of Hec1 knockdown as well. The mitotic index of Hec1 RNAi (12.9±2.3%) was similar to that of ASURA RNAi (Fig. 1B). The advantage of employing Hec1 RNAi is that, among the kinetochore proteins that we have tested, Hec1 has been studied the most regarding its function at the kinetochore. DeLuca *et al.* [13] showed by using EM that Hec1 and Nuf2 localized at the kinetochore outer layer. As the structural effect of Nuf2 RNAi (Hec1 is depleted at the same time) is well studied, Hec1 was used as a model protein throughout this study.

We next assessed the role of ASURA on mitotic progression. Cultures subjected to ASURA siRNA treatment displayed a high percentage of prometaphase cells (82.0±2.5%), more than double the control (36.9±3.1%) (Fig. 1C). There were only a few cells with chromosomes aligned in the metaphase plate (Fig. 1C, D), with most of the mitotic cells showing non-alignment or misalignment.

Decreased kinetochore localization of Hec1 and CENP-F correlates with chromosome misalignment in ASURA repression

When we examined for ASURA localization profile, immunofluorescence showed that ASURA is predominantly localized at the cytoplasm (Fig. 1E), as revealed by expression of GFP-ASURA [45]. Unlike Hec1, which localized to the kinetochore during mitotic phase, there was no obvious signal of ASURA localization specifically to the kinetochore or centromeric region throughout the cell cycle, indicating that ASURA is not a kinetochore component. Next, we investigated ASURA effect on kinetochore proteins localization. In mock transfected cultures, Hec1 (Figs. 1E, 2B) and CENP-F (Fig. 2A) localized normally at the kinetochore. With partial depletion of ASURA, kinetochore localization of CENP-F (Fig. 2A, C) was abolished, whereas Hec1 intensity decreased to 50% of the control (Fig. 2B, C), consistent with our previous report [45]. Hec1 expression level was unaltered in the absence of ASURA (Fig. 1A), indicating that this is not an off-target effect.

We confirmed premature sister chromatid separation (Fig. 2B) after knockdown of ASURA [45]. Interestingly, we found that even in Hec1 knockdown cultures, sister chromatids were separated in about 30% of the cells, which has not been reported elsewhere (Fig. 2B). The exact reason for this separation remains obscure (refer to discussion), although this is observed only in cells with Hec1 intensity lower than 5% of the normal (Fig. 3). The possibility that the loss of sister chromatid cohesion in ASURA partial depletion was due to the lower levels of Hec1 was not apparent from our data. In particular, when Hec1 intensity at the kinetochore is about 50% of the control, a level similar to that of ASURA disruption, sister chromatids were rarely separated.

Combining all the data [45], ASURA is required for kinetochore localization of Hec1, CENP-F, and also CENP-E. Thus, we suggest that ASURA depletion leads to improper kinetochore assembly.

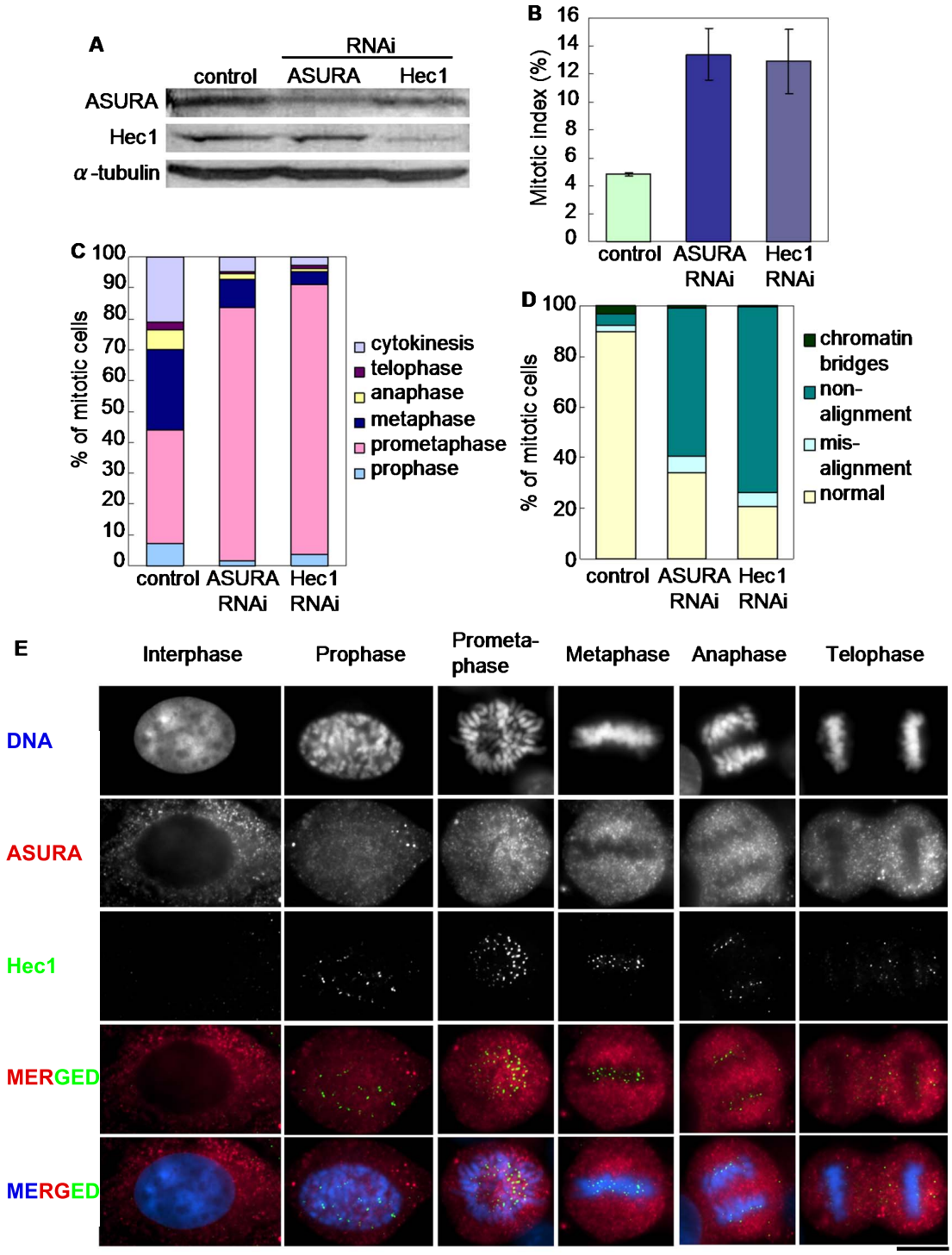

Fig. 1. Abnormal chromosome congression and mitotic defects associated with ASURA partial depletion and ASURA localization throughout the cell cycle. (**A**) Partial depletion of ASURA and Hec1 by RNAi treatment. α-tubulin was used as loading control. (**B**) Mitotic indexes of ASURA and Hec1 knockdown cells (n >1000). Three independent experiments were performed for each set of treatment. (**C**) Percentages of each mitotic phase of ASURA and Hec1 RNAi cells. (**D**) Distortion of chromosome alignment in ASURA and Hec1 knockdown cells. Misalignment represents cells with ≤10 unaligned chromosomes at the metaphase plate and nonalignment represents cells with >10 unaligned chromosomes. (**E**) ASURA localized to both cytoplasm and nucleus during interphase. In prophase and prometaphase, ASURA localized to chromosomes and cytoplasm, but was mainly cytoplasmic from metaphase until the end of the mitotic phase, although some signals were detected at the chromosomes. Bar=10 μm.

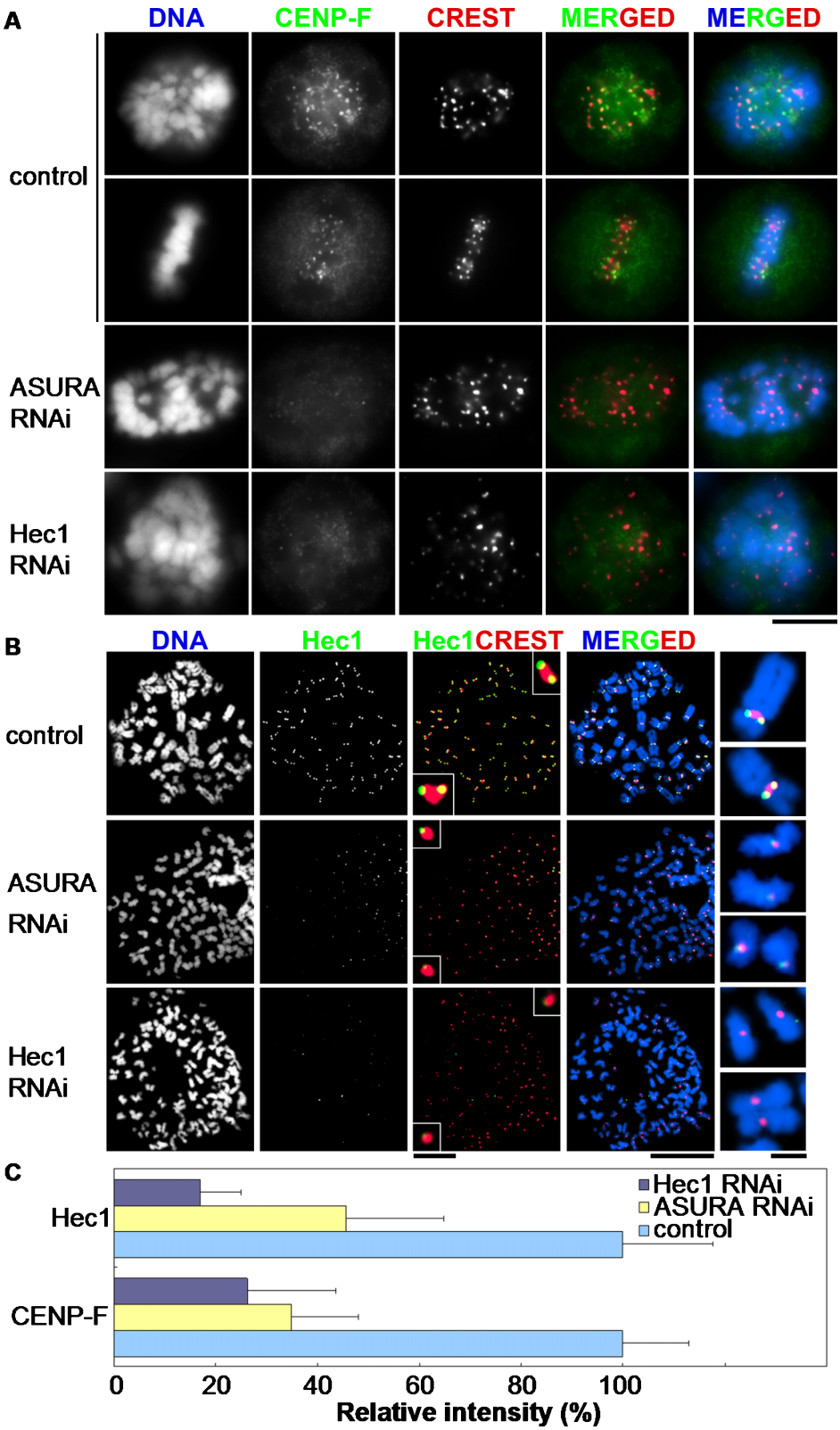

Fig. 2. ASURA knockdown cells showed reduction of CENP-F and Hec1 at kinetochore and defects in sister chromatid cohesion. (**A**) Signal intensity of CENP-F was diminished after both ASURA and Hec1 RNAi. (**B**) Signal intensity of Hec1 was decreased after both ASURA and Hec1 RNAi. Most of the chromatids lost their cohesion in both ASURA and Hec1 RNAi. (**A, B**) Bars=10 μm, 2 μm (insets). (**C**) Quantitative measurement of signal intensities of Hec1 and CENP-F.

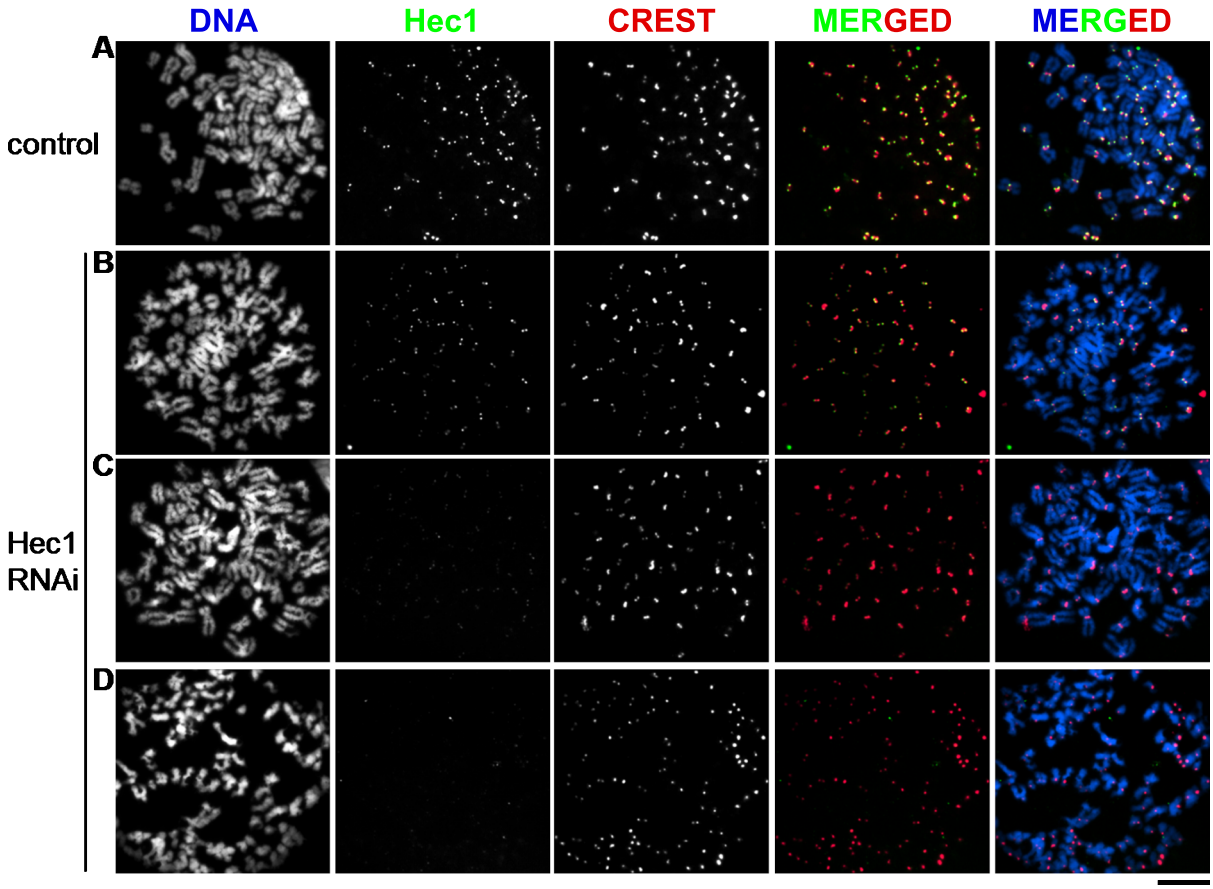

Fig. 3. Sister chromatid separation in Hec1 knockdown cells. (**A**) Control. (**B–D**) Hec1 partially depleted cells. Signal intensities of Hec1 were normalized to those of the control. (**B**) 50% of Hec1 intensity. (**C**) 10% of Hec1 intensity. Sister chromatids were not separated. (**D**) 5% of Hec1 intensity. Sister chromatids were separated. Bar=10 μm.

Kinetochore assembly is divided into three stages

To confirm the above hypothesis, we adopted electron microscopy for our RNAi analyses. As the defects observed in kinetochore may be derived from the disruption of the maturation process, we first ascertained the kinetochore development in HeLa cells. Figure 4A showed a prophase cell. The nuclear envelope (green arrows) and nucleoli (red arrowheads) are visible. Kinetochores were observed as either a fibrous mass (Fig. 4B, D, blue arrows) or fuzzy ball with a partially constructed kinetochore plate (Fig. 4B, C, red arrows). After nuclear envelope breakdown, the outer plates became clearer and began to interact with MTs. Figure 4E shows a pair of sister kinetochores from a chromosome located near the metaphase plate in a prometaphase cell. The right one is interacting end-on with the robust kinetochore MTs, although the plate structure is less obvious. The kinetochore at the left is interacting side-on with a MT running close-by, and the fibrous corona (blue arrowheads in Fig. 4E) is visible [14]. During prometaphase, kinetochores facing the poles are favorable in capturing MTs [43]. Once this association is established, kinetochores were transported poleward via the corona [43], forming lateral interactions with any stabilized MT bundles [5]. Even if chromosomes fail to achieve bi-orientation at the poles, the chromosomes glide along the kinetochore fibers with the aid of CENP-E from the corona to obtain bi-orientation at the metaphase plate [21], which is known as the mono-oriented pathway [5]. In the prometaphase, some kinetochores remained as fuzzy balls without internal structure (data not shown).

The final step of the maturation is achieved when the electron-dense outer plate and inner plate are completely formed, enabling the kinetochore to capture robust MTs and achieve bi-orientation (Fig. 4F) by the end of prometaphase. A schematic model showing the development of the kinetochore is presented based on the observations above (Fig. 4G). Kinetochores are classified into three developmental groups, Class 1, 2, and 3.

Defective kinetochore-MT attachment in ASURA RNAi derived from immature kinetochore development

Mock transfected control (Fig. 5A), ASURA RNAi (Fig. 5B) and Hec1 RNAi (Fig. 5C) cells were analyzed under the aforementioned conditions. Kinetochores were classified by referring to their maturation process (Fig. 4G). The quantitative data are shown in Figure 5M. Normally,

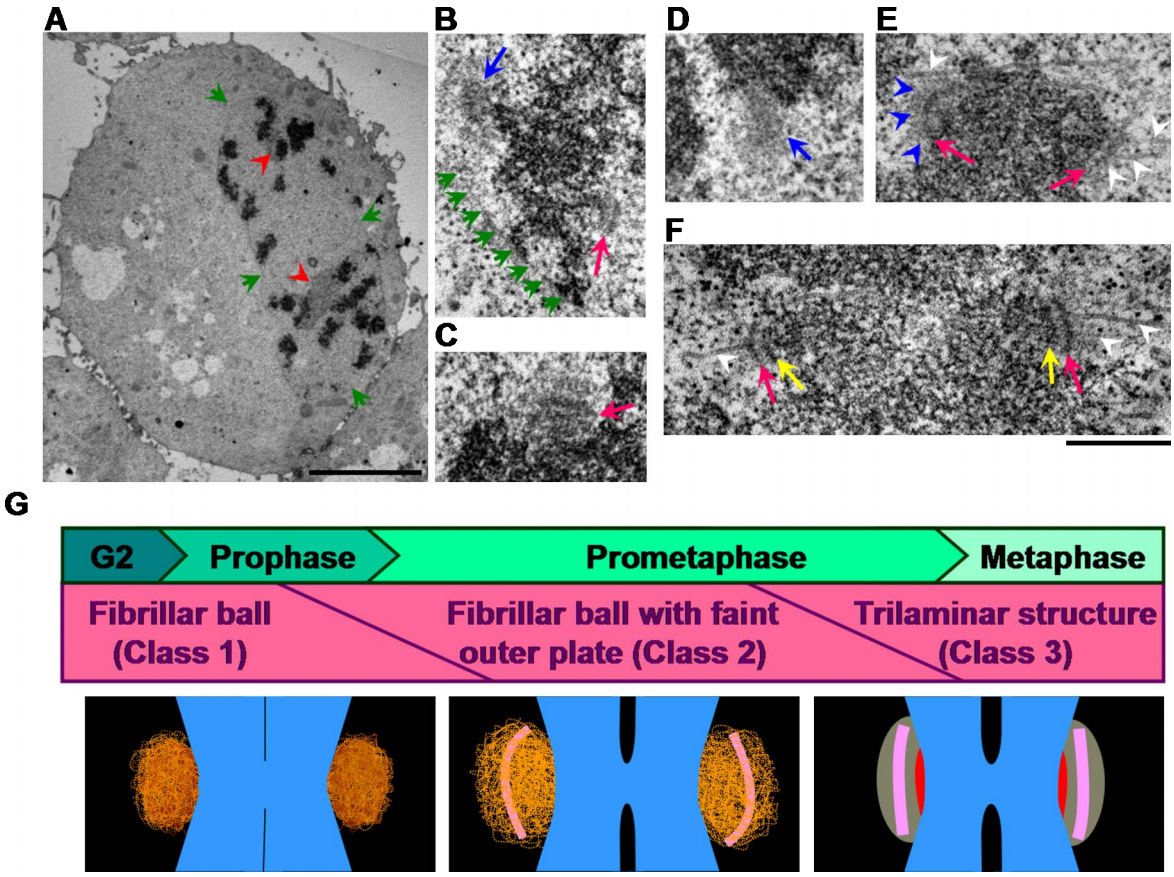

Fig. 4. Kinetochore maturation revealed by EM and its schematic representation. (**A**) Low magnification electron micrograph of a prophase cell. Nuclear envelope (green arrows) and two nucleoli (red arrowheads) are visible. Bar=5 μm. (**B–D**) Kinetochores at prophase, either showing the ambiguous outer plates (red arrows) or fibrillar balls (blue arrows). No kinetochore-MT was detected. Nuclear envelope is shown by green arrows. (**E**) Prometaphase kinetochores retaining the fibrillar balls with the faint outer plates (red arrows). MTs (white arrowheads) interact end-on with the right kinetochore. The left kinetochore interacts laterally with a microtubule. Fibrous corona (blue arrowheads) is visible. (**F**) The mature and bi-oriented kinetochores observed at early anaphase. The conspicuous inner layers (yellow arrows) and outer plates (red arrows) were separated by an electron-lucent middle layer. Robust MTs (white arrowheads) with end-on attachment were detected. Scale bars are 500 nm. (**G**) A schematic model of kinetochore development. Kinetochore maturation is classified into 3 groups, Class 1, 2, or 3 based on their morphology. The maturation process occurs in parallel with chromosome condensation during mitosis. MTs were eliminated from the figure to avoid complexity.

Class 3 kinetochores form the majority, more than 75% of the population, as shown in the control. This is rarely the case in the ASURA and Hec1 RNAi cultures, where less than 10% are classified as Class 3. DeLuca *et al.* [13] showed that in Nuf2-Hec1 depletion, more than 50% of the kinetochores observed failed to form a well-recognized outer plate. Liu *et al.* [25] also revealed that fuzzy balls were frequently observed in the absence of Nuf2. We made a similar observation for Hec1 RNAi, where highly disorganized kinetochores were significantly increased (Fig. 5M, Class 1). As expected, kinetochore outer plates were either undeveloped (Class 1) or poorly-formed (Class 2) with the partial depletion of ASURA. Even when a layered structure was constructed, the outer plates, and sometimes even the inner plates, were often pulled out or stretched (Fig. 5H, I), indicating that without ASURA the kinetochore lacks physical rigidity against the MT pulling forces, although MT attachments were less frequent compared to the authentic trilaminar structure (Fig. 5D). The morphological defects observed in ASURA knockdown cultures were similar to those of Hec1 disruption (Fig. 5J–L). This suggests that the abnormalities observed in kinetochore formation derived from the effect of mislocalization of Hec1 and other outer kinetochore proteins downstream. Altogether, this clearly shows that ASURA is an essential protein for proper kinetochore formation, most probably by targeting kinetochore proteins.

IV. Discussion

We confirmed that mitotic defects were rescued by expressing RNAi-refractory ASURA plasmid in the same RNAi condition. We also confirmed that ASURA RNAi cells were arrested in prometaphase or metaphase, in addition

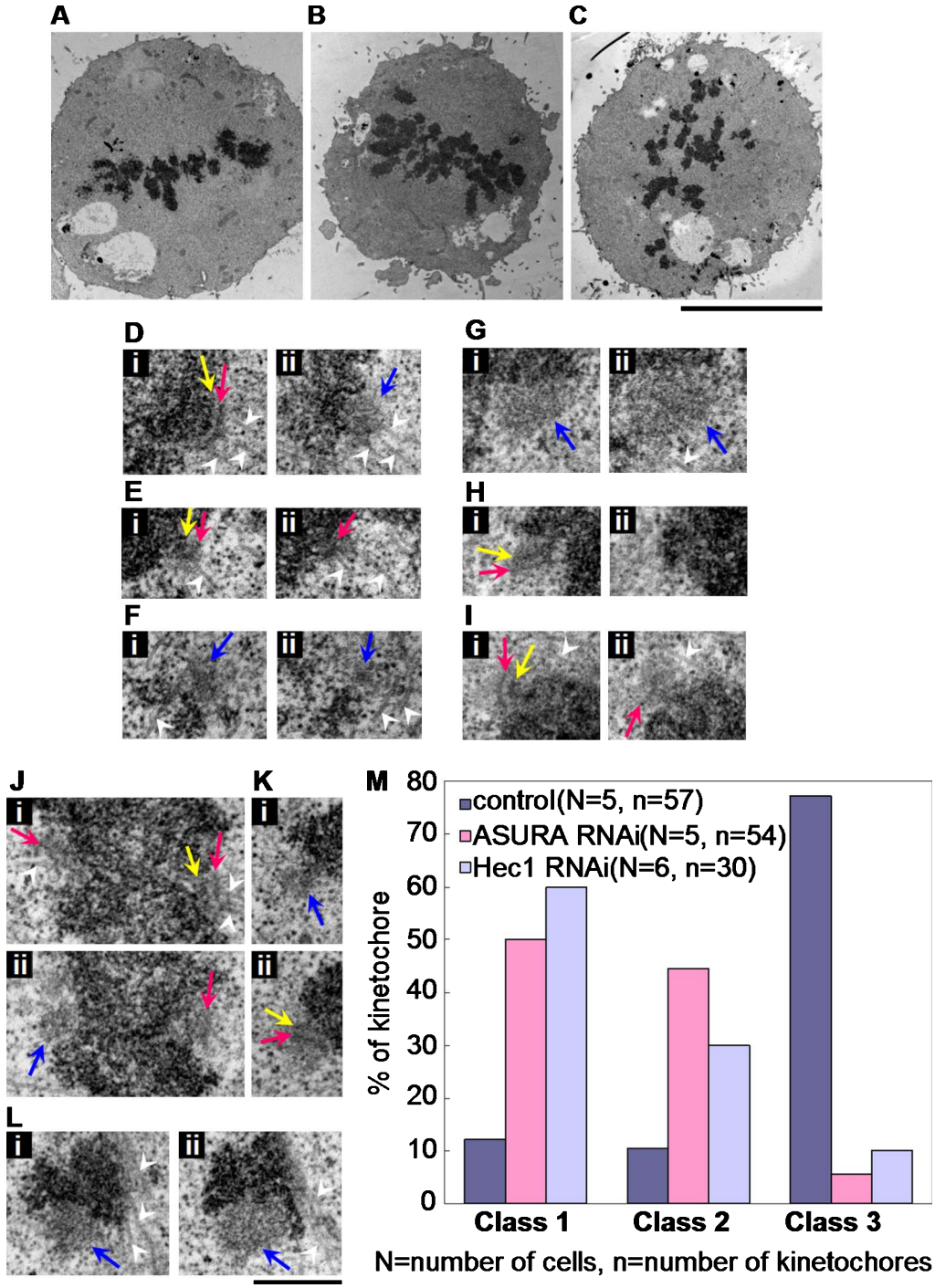

Fig. 5. Electron micrographs of ASURA and Hec1 knockdown cells. (**A**) Mitotic metaphase cell as the control. (**B**) ASURA RNAi cell. (**C**) Hec1 RNAi cell. Bar=10 μm. (**D–L**) ASURA partial depletion resulted in kinetochore assembly disorder. Adjacent serial sections are indicated as i and ii. Red and yellow arrows show the outer plates and the inner plates, respectively. Blue arrows show the kinetochore with fuzzy appearance. White arrowheads indicate MTs. (**D–F**) Serial sections of kinetochores from the control. (**D**) Trilaminar kinetochores with MT attachment, classified as Class 3 kinetochore. (**E**) Example of an immature kinetochore with a faint outer plate (Class 2). (**F**) Kinetochore with fibrillar ball appearance (Class 1). (**G–I**) Kinetochores in ASURA partially depleted cells. (**G**) Kinetochore showed the fuzzy ball structure (Class 1). (**H, I**) Despite kinetochore plates being partially formed, they were stretched and/or pulled out from the chromosome body (Class 2). (**J–L**) Kinetochores in Hec1 RNAi cultures. (**J, K**) Kinetochore plates were partially formed (Class 2), but were stretched or pulled out from the chromosome body as in ASURA RNAi. Even the inner plates seem to be partially pulled off from the centromere (also observed in **H, I**). (**L**) Class 1 kinetochore. All micrographs are shown in the same magnification. Bar=500 nm. (**M**) Kinetochores in each treatment were classified into Class 1, 2, or 3 based on their structure. In ASURA and Hec1 RNAi, the majority of the kinetochore plates were either poorly-formed (Class 2) or unrecognized (Class 1).

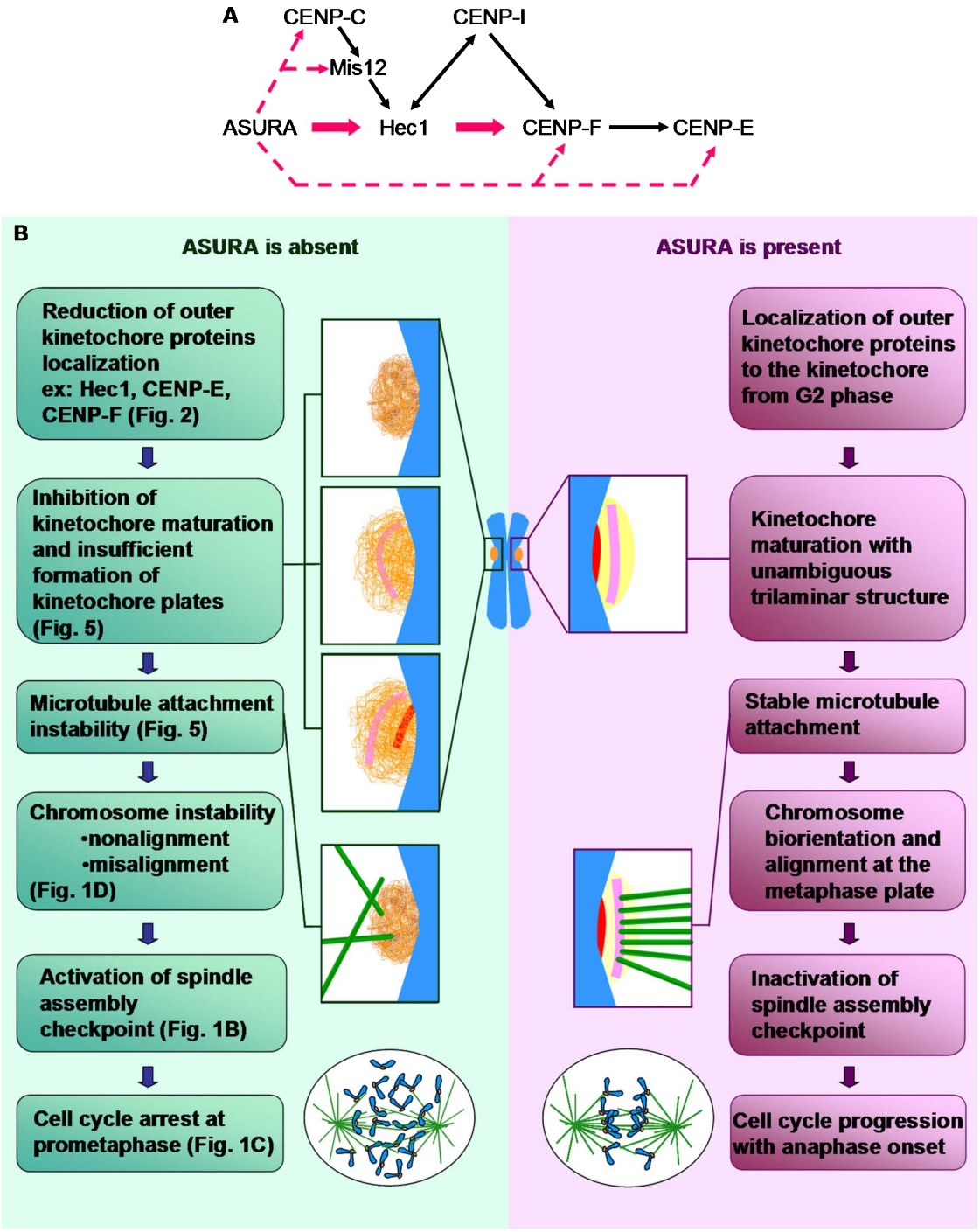

Fig. 6. Roles of ASURA for kinetochore assembly and subsequent chromosome congression. (**A**) ASURA recruits Hec1 and then CENP-F to kinetochores (red arrows). CENP-I recruits Hec1 and CENP-F through two distinct pathways, and Hec1 has a negative feedback effect to CENP-I. CENP-C recruits Mis12 and subsequently Hec1 to the kinetochore (black arrows) [25]. Dotted lines indicate putative pathways for kinetochore assembly. (**B**) Schematic models presenting kinetochore maturation. Left: Each step of immature kinetochore development and chromosome nonalignment as a result. Right: Each step of authentic kinetochore maturation and chromosome segregation.

to its role in the regulation of sister chromatid cohesion, proper mitotic spindle formation, and localization of some kinetochore proteins, and activates the spindle assembly checkpoint [45]. In this study, we further examined the mechanism underlying disruption of the stable kinetochore-MT attachment establishment in ASURA RNAi. When investigated under EM, only a few kinetochore-MTs were detected in the ASURA knockdown cells, and even less in those depleted of Hec1. MT associations were not completely abolished, because MT interactions were detected,

although they were not stable and were probably transient. This is consistent with our previous report that cold-stable MTs do not persist in cells lacking ASURA, similar to those of Hec1 RNAi [45]. Decreased levels of outer kinetochore proteins are likely to contribute to the abnormalities observed in kinetochore formation when ASURA is partially depleted. It is noteworthy that ASURA has neither been shown to specifically localize at the kinetochore nor has been identified as a kinetochore protein in proteome analyses of several model organisms tested [1, 36, 44, 49], nor even has been reported to interact with any kinetochore protein. ASURA is a component of the highly purified metaphase chromosomes [49]. Recent proteome analysis using purified DT40 chromosomes identified 4000 proteins, which were classified into 28 classes [36]. Prohibitin was classified as a contaminant from the mitochondria and cytoplasm, although it was not specified which subunit of the prohibitin complex this referred to.

This is the main reason why ASURA is so unique in the kinetochore assembly. ASURA associates with chromatin in G2 phase (data not shown), and is slightly enriched at the chromosome mainly during prophase and prometaphase (Fig. 1E). Hec1 [25] and CENP-F [24] assemble at the kinetochore during late G2, while CENP-E assembles onto the kinetochore slightly after the nuclear envelope breakdown [52]. Further investigation on how ASURA interacts with the kinetochore proteins may be revealed by their ultrastructural localization analyses [28, 48]. The kinetochore phenotypes of ASURA partial depletion are similar to that of Hec1 and CENP-F depletion; this, together with the fact of their mislocalization after ASURA knockdown, suggests that the defects observed in kinetochore assembly were indirect, where ASURA is required for targeting one or more of these proteins to the kinetochore, and that the failure to do so in turn leads to improper kinetochore development. When we partially depleted Hec1 from the cells, CENP-F was largely diminished, consistent with the results obtained by Miller *et al.* [32]. Although some contradictions remain regarding CENP-E recruitment, our data suggested that the reduction of kinetochore outer plate proteins after ASURA depletion is derived from the Hec1-CENP-F pathway, and subsequently CENP-E (Fig. 6A).

CENP-I and CENP-C are required for Hec1 localization, in two independent pathways [25]. ASURA may be involved in one or both of the pathways, or may also form another completely different pathway from those that have already been reported, to localize and/or maintain Hec1 at the kinetochore. Whether ASURA affects the inner kinetochore formation has yet to be determined, because inner kinetochore plates with some defects (e.g. pulled-away from the centromere) were detected more frequently in ASURA RNAi than in Hec1 RNAi. However, this can also be explained by the greater degree of disorganization in the kinetochore lacking Hec1, compare to that of ASURA RNAi.

Something else that intrigued us was that Hec1 partial depletion also led to premature sister chromatid separation. It has been reported by Holt *et al.* [19] that CENP-F repression weakens centromeric cohesion in about 28% of metaphase spread chromosomes, which is similar to our Hec1 RNAi, where CENP-F intensities at the kinetochores were less than 25% of the control. These results suggest the possibility that loss of sister chromatid cohesion with Hec1 RNAi recapitulate partially, if not all, the phenotypes in decreased levels of CENP-F. Alternatively, two independent studies indicated that Hec1 localization at the kinetochore is crucial for checkpoint activation, and mitotic arrest is abrogated when Hec1 is totally depleted from the kinetochore [30, 42]. Therefore, it is also feasible that the cells with premature loss of sister chromatid cohesion were indeed cells that had overridden the mitotic checkpoint and entered anaphase as the Hec1 levels were very low. A recent study published during our manuscript preparation indicated another possibility for the untimely sister chromatid separation, referred to as cohesion fatigue, which is due to prolonged mitotic arrest [12]. Whether this is the case in Hec1 RNAi is unknown, because stable microtubule interactions were very few, whereas cohesion fatigue required microtubule pulling forces.

In summary, ASURA is essential for chromosome congression, due to its important role in facilitating kinetochore assembly and regulating sister chromatid cohesion. Mitotic arrest with ASURA knockdown is largely derived from the failure of kinetochore outer plate formation, resulting in poor kinetochore-MT attachment (Fig. 6B). Kinetochore proteins, except for CENP-A where HJURP serves as its deposition factor [15, 17], are known to be recruited by other kinetochore proteins upstream [6, 9, 25]. Thus, the underlying mechanism should be carefully investigated, as this is the first protein reported to be required for both kinetochore assembly and cohesion, but which does not show any specific localization at the centromere region.

V. Acknowledgments

A part of the present experiments was carried out by using a facility in the Research Center for Ultrahigh Voltage Electron Microscopy, Osaka University. We are especially grateful for the excellent technical support of Dr. Tomoki Nishida and Mr. Toshiaki Hasegawa. We are also indebted to Associate Prof. Sumire Inaga and Dr. Tetsuo Katsumoto of the Faculty of Medicine, Tottori University for their helpful advice and for sharing the protocols of electron microscopy. This work was supported by the Grants-in-Aid for Scientific Research from the Ministry of Education, Culture, Sports, Science and Technology of Japan (MEXT, No. 21248040, to K.F). M.H.L. would also like to thank MEXT for fellowship support.

VI. References

1. Akiyoshi, B., Nelson, C. R., Ranish, J. A. and Biggins, S. (2009) Quantitative proteomic analysis of purified yeast kinetochores identifies a PP1 regulatory subunit. *Genes Dev.* 23; 2887–2899.

2. Artal-Sanz, M. and Tavernarakis, N. (2009) Prohibitin and mitochondrial biology. *Trends Endocrinol. Metab.* 20; 394–401.
3. Brinkley, B. R. and Stubblefield, E. (1966) The fine structure of the kinetochore of a mammalian cell *in vitro*. *Chromosoma* 19; 28–43.
4. Brinkley, B. R., Valdivia, M. M., Tousson, A. and Balczon, R. D. (1989) The kinetochore: structure and molecular organization. In "Mitosis: Molecules and Mechanisms", ed. by J. S. Hyams and B. R. Brinkley. Academic Press, New York, pp. 77–118.
5. Cai, S., O'Connell, C. B., Khodjakov, A. and Walczak, C. E. (2009) Chromosome congression in the absence of kinetochore fibres. *Nat. Cell Biol.* 11; 832–838.
6. Chan, G. K., Liu, S. T. and Yen, T. J. (2005) Kinetochore structure and function. *Trends Cell Biol.* 15; 589–598.
7. Cheeseman, I. M., Anderson, S., Jwa, M., Green, E. M., Kang, J., Yates, J. R. III., Drubin, D. G. and Barnes, G. (2002) Phospho-regulation of kinetochore-MT attachments by the Aurora kinase Ipl1p. *Cell* 111; 163–172.
8. Cheeseman, I. M., Niessen, S., Anderson, S., Hyndman, F., Yates, J. R. III. and Desai, A. (2004) A conserved protein network controls assembly of the outer kinetochore and its ability to sustain tension. *Genes Dev.* 18; 2255–2268.
9. Cheeseman, I. M. and Desai, A. (2008) Molecular architecture of the kinetochore-microtubule interface. *Nat. Rev. Mol. Cell Biol.* 9; 33–46.
10. Cleveland, D. W., Mao, Y. and Sullivan, K. F. (2003) Centromeres and kinetochores: from epigenetics to mitotic checkpoint signaling. *Cell* 112; 407–421.
11. Comings, D. E. and Okada, T. A. (1971) Fine structure of kinetochore in Indian muntjac. *Exp. Cell Res.* 67; 97–110.
12. Daum, J. R., Potapova, T. A., Sivakumar, S., Daniel, J. J., Flynn, J. N., Rankin, S. and Gorbsky, G. J. (2011) Cohesion fatigue induces chromatid separation in cells delayed at metaphase. *Curr. Biol.* 21; 1018–1024.
13. DeLuca, J. G., Dong, Y., Hergert, P., Strauss, J., Hickey, J. M., Salmon, E. D. and McEwen, B. F. (2005) Hec1 and Nuf2 are core components of the kinetochore outer plate essential for organizing microtubule attachment sites. *Mol. Biol. Cell* 16; 519–531.
14. Dong, Y., Vanden Beldt, K. J., Meng, X., Khodjakov, A. and McEwen, B. F. (2007) The outer plate in vertebrate kinetochores is a flexible network with multiple microtubule interactions. *Nat. Cell Biol.* 9; 516–522.
15. Dunleavy, E. M., Roche, D., Tagami, H., Lacoste, N., Ray-Gallet, D., Nakamura, Y., Daigo, Y., Nakatani, Y. and Almouzni-Pettinotti, G. (2009) HJURP is a cell-cycle-dependent maintenance and deposition factor of CENP-A at centromeres. *Cell* 137; 485–497.
16. Foltz, D. R., Jansen, L. E., Black, B. E., Bailey, A. O., Yates, J. R. III and Cleveland, D. W. (2006) The human CENP-A centromeric nucleosome-associated complex. *Nat. Cell Biol.* 8; 458–469.
17. Foltz, D. R., Jansen, L. E., Bailey, A. O., Yates, J. R. III, Wood, S., Black, B. E. and Cleveland, D. W. (2009) Centromere-specific assembly of CENP-A nucleosomes is mediated by HJURP. *Cell* 137; 472–484.
18. Fusaro, G., Dasgupta, P., Rastogi, S., Joshi, B. and Chellappan, S. (2003) Prohibitin induces the transcriptional activity of p53 and is exported from the nucleus upon apoptotic signaling. *J. Biol. Chem.* 278; 47853–47861.
19. Holt, S. V., Vergnolle, M. A., Hussein, D., Wozniak, M. J., Allan, V. J. and Taylor, S. S. (2005) Silencing CENP-F weakens centromeric cohesion, prevents chromosome alignment and activates the spindle checkpoint. *J. Cell Sci.* 118; 4889–4900.
20. Joglekar, A. P., Bloom, K. and Salmon, E. D. (2009) In vivo protein architecture of the eukaryotic kinetochore with nanometer scale accuracy. *Curr. Biol.* 19; 694–699.
21. Kapoor, T. M., Lampson, M. A., Hergert, P., Cameron, L., Cimini, D., Salmon, E. D., McEwen, B. F. and Khodjakov, A. (2006) Chromosomes can congress to the metaphase plate before biorientation. *Science* 311; 388–391.
22. Kasashima, K., Ohta, E., Kagawa, Y. and Endo, H. (2006) Mitochondrial functions and estrogen receptor-dependent nuclear translocation of pleiotropic human prohibitin 2. *J. Biol. Chem.* 281; 36401–36410.
23. Kurtev, V., Margueron, R., Kroboth, K., Ogris, E., Cavailles, V. and Seiser, C. (2004) Transcriptional regulation by the repressor of estrogen receptor activity via recruitment of histone deacetylases. *J. Biol. Chem.* 279; 24834–24843.
24. Liao, H., Winkfein, R. J., Mack, G., Rattner, J. B. and Yen, T. J. (1995) CENP-F is a protein of the nuclear matrix that assembles onto kinetochores at late G2 and is rapidly degraded after mitosis. *J. Cell Biol.* 130; 507–518.
25. Liu, S. T., Rattner, J. B., Jablonski, S. A. and Yen, T. J. (2006) Mapping the assembly pathways that specify formation of the trilaminar kinetochore plates in human cells. *J. Cell Biol.* 175; 41–53.
26. Ma, N., Matsunaga, S., Takata, H., Ono-Maniwa, R., Uchiyama, S. and Fukui, K. (2007) Nucleolin functions in nucleolus formation and chromosome congression. *J. Cell Sci.* 120; 2091–2105.
27. Martin-Lluesma, S., Stucke, V. M. and Nigg, E. A. (2002) Role of Hec1 in spindle checkpoint signaling and kinetochore recruitment of Mad1/Mad2. *Science* 297; 2267–2270.
28. Matsuzaki, T., Hata, H., Ozawa, H. and Takata, K. (2009) Immunohistochemical localization of the aquaporins AQP1, AQP3, AQP4, and AQP5 in the mouse respiratory system. *Acta Histochem. Cytochem.* 42; 159–169.
29. McClung, J. K., Danner, D. B., Stewart, D. A., Smith, J. R., Schneider, E. L., Lumpkin, C. K., Dell'Orco, R. T. and Nuell, M. J. (1989) Isolation of a cDNA that hybrid selects antiproliferative mRNA from rat liver. *Biochem. Biophys. Res. Commun.* 164; 1316–1322.
30. Meraldi, P., Draviam, V. M. and Sorger, P. K. (2004) Timing and checkpoints in the regulation of mitotic progression. *Dev. Cell* 7; 45–60.
31. Merkwirth, C. and Langer, T. (2009) Prohibitin function within mitochondria: essential roles for cell proliferation and cristae morphogenesis. *Biochim. Biophys. Acta* 1793; 27–32.
32. Miller, S. A., Johnson, M. L. and Stukenberg, P. T. (2008) Kinetochore attachments require an interaction between unstructured tails on microtubules and Ndc80 (Hec1). *Curr. Biol.* 18; 1785–1791.
33. Mitchison, T. J. (1988) Microtubule dynamics and kinetochore function in mitosis. *Annu. Rev. Cell Biol.* 4; 527–549.
34. Montano, M. M., Ekena, K., Delage-Mourroux, R., Chang, W., Martini, P. and Katzenellenbogen, B. S. (1999) An estrogen receptor-selective coregulator that potentiates the effectiveness of antiestrogens and represses the activity of estrogens. *Proc. Natl. Acad. Sci. U S A* 96; 6947–6952.
35. Nicklas, R. B. (1989) The motor for poleward chromosome movement in anaphase is in or near the kinetochore. *J. Cell Biol.* 109; 2245–2255.
36. Ohta, S., Bukowski-Wills, J. C., Sanchez-Pulido, L., Alves Fde, L., Wood, L., Chen, Z. A., Platani, M., Fischer, L., Hudson, D. F., Ponting, C. P., Fukagawa, T., Earnshaw, W. C. and Rappsilber, J. (2010) The protein composition of mitotic chromosomes determined using multiclassifier combinatorial proteomics. *Cell* 142; 810–821.
37. Ribeiro, S. A., Vagnarelli, P., Dong, Y., Hori, T., McEwen, B. F., Fukagawa, T., Flors, C. and Earnshaw, W. C. (2010) A super-resolution map of the vertebrate kinetochore. *Proc. Natl. Acad. Sci. U S A* 107; 10484–10489.
38. Rieder, C. L. (1982) The formation, structure, and composition of the mammalian kinetochore and kinetochore fiber. *Int. Rev. Cytol.*

79; 1–58.
39. Rieder, C. L. and Alexander, S. P. (1990) Kinetochores are transported poleward along a single astral microtubule during chromosome attachment to the spindle in newt lung cells. *J. Cell Biol.* 110; 81–95.
40. Roos, U. P. (1973) Light and electron microscopy of rat kangaroo cells in mitosis. II. Kinetochore structure and function. *Chromosoma* 41; 195–220.
41. Santaguida, S. and Musacchio, A. (2009) The life and miracles of kinetochores. *EMBO J.* 28; 2511–2531.
42. Saurin, A. T., van der Waal, M. S., Medema, R. H., Lens, S. M. and Kops, G. J. (2011) Aurora B potentiates Mps1 activation to ensure rapid checkpoint establishment at the onset of mitosis. *Nat. Commun.* 2; 316.
43. Schvartzman, J. M., Sotillo, R. and Benezra, R. (2010) Mitotic chromosomal instability and cancer: mouse modelling of the human disease. *Nat. Rev. Cancer* 10; 102–115.
44. Takata, H., Uchiyama, S., Nakamura, N., Nakashima, S., Kobayashi, S., Sone, T., Kimura, S., Lahmers, S., Granzier, H., Labeit, S., Matsunaga, S. and Fukui, K. (2007) A comparative proteome analysis of human metaphase chromosomes isolated from two different cell lines reveals a set of conserved chromosome-associated proteins. *Genes Cells* 12; 269–284.
45. Takata, H., Matsunaga, S., Morimoto, A., Ma, N., Kurihara, D., Ono-Maniwa, R., Nakagawa, M., Azuma, T., Uchiyama, S. and Fukui, K. (2007) PHB2 protects sister-chromatid cohesion in mitosis. *Curr. Biol.* 17; 1356–1361.
46. Tanaka, T. U. (2005) Chromosome bi-orientation on the mitotic spindle. *Philos. Trans. R. Soc. Lond. B. Biol. Sci.* 360; 581–589.
47. Tatsuta, T., Model, K. and Langer, T. (2005) Formation of membrane-bound ring complexes by prohibitins in mitochondria. *Mol. Biol. Cell* 16; 248–259.
48. Tsukioka, F., Wakayama, T., Tsukatani, T., Miwa, T., Furukawa, M. and Iseki, S. (2007) Expression and localization of the cell adhesion molecule SgIGSF during regeneration of the olfactory epithelium in mice. *Acta Histochem. Cytochem.* 40; 43–52.
49. Uchiyama, S., Kobayashi, S., Takata, H., Ishihara, T., Hori, N., Higashi, T., Hayashihara, K., Sone, T., Higo, D., Nirasawa, T., Takao, T., Matsunaga, S. and Fukui, K. (2005) Proteome analysis of human metaphase chromosomes. *J. Biol. Chem.* 280; 16994–17004.
50. Wan, X., O'Quinn, R. P., Pierce, H. L., Joglekar, A. P., Gall, W. E., DeLuca, J. G., Carroll, C. W., Liu, S. T., Yen, T. J., McEwen, B. F., Stukenberg, P. T., Desai, A. and Salmon, E. D. (2009) Protein architecture of the human kinetochore microtubule attachment site. *Cell* 137; 672–684.
51. Wise, D., Cassimeris, L., Rieder, C. L., Wadsworth, P. and Salmon, E. D. (1991) Chromosome fiber dynamics and congression oscillations in metaphase PtK2 cells at 23 degrees C. *Cell Motil. Cytoskel.* 18; 1313–1342.
52. Yen, T. J., Compton, D. A., Wise, D., Zinkowski, R. P., Brinkley, B. R., Earnshaw, W. C. and Cleveland, D. W. (1991) CENP-E, a novel human centromere-associated protein required for progression from metaphase to anaphase. *EMBO J.* 10; 1245–1254.
53. Zinkowski, R. P., Meyne, J. and Brinkley, B. R. (1991) The centromere-kinetochore complex: a repeat subunit model. *J. Cell Biol.* 113; 1091–1110.